ISSN 1070-3284, Russian Journal of Coordination Chemistry, 2022, Vol. 48, No. 7, pp. 422–429. © Pleiades Publishing, Ltd., 2022.
Russian Text © The Author(s), 2022, published in Koordinatsionnaya Khimiya, 2022, Vol. 48, No. 7, pp. 414–421.

The authors congratulate Academician V. I. Ovcharenko on the 70th birthday

Generation of Long-Lived Phenoxyl Radical in the Binuclear Copper(II) Pivalate Complex with 2,6-Di-*tert*-butyl-4-(3,5-bis(4-pyridyl)pyridyl)phenol

V. N. Dorofeeva[a], A. V. Pavlishchuk[a, b], M. A. Kiskin[c, *], N. N. Efimov[c], V. V. Minin[c], K. S. Gavrilenko[b, d], S. V. Kolotilov[a], V. V. Pavlishchuk[a], and I. L. Eremenko[c, e]

[a] *Pisarzhevsky Institute of Physical Chemistry, National Academy of Sciences of Ukraine, Kyiv, Ukraine*
[b] *Taras Shevchenko National University of Kyiv, Kyiv, Ukraine*
[c] *Kurnakov Institute of General and Inorganic Chemistry, Russian Academy of Sciences, Moscow, Russia*
[d] *Enamine Research and Production Association, Kyiv, Ukraine*
[e] *Nesmeyanov Institute of Organoelement Compounds, Russian Academy of Sciences, Moscow, Russia*
**e-mail: mkiskin@igic.ras.ru*

Received December 15, 2021; revised December 24, 2021; accepted December 27, 2021

Abstract—A new binuclear copper(II) complex $Cu_2(Piv)_4(L)_2$, where Piv^- = pivalate, L = 2,6-di-*tert*-butyl-4-(3,5-bis(4-pyridyl)pyridyl)phenol, was synthesized, and its molecular and crysral structures were determined at temperatures of 160, 173, and 296 K (CIF files CCDC no. 2144104, 2144105, and 2144106, respectively). Cyclic voltammetry measurements revealed three irreversible oxidation processes in the potential range of 0.5–1.2 V versus Fc^+/Fc. Analysis of the temperature dependence of the magnetic susceptibility of $Cu_2(Piv)_4(L)_2$ showed that antiferromagnetic interactions of Cu^{2+} ions predominate in the complex. It was found that the oxidation of $Cu_2(Piv)_4(L)_2$ upon grinding with PbO_2 or treatment of a solid sample with an aqueous solution of $K_3[Fe(CN)_6]$ affords long-lived phenoxyl radical, which can be detected by ESR spectroscopy.

Key words: binuclear complex, copper, carboxylates, phenoxyl radical, magnetic properties, redox properties

DOI: 10.1134/S1070328422070041

Transition metal complexes in which minor changes of the chemical composition due to reactions with other compounds or external stimuli induce significant changes in physical characteristics are considered as a basis for the design of new molecular magnets [1–3], multifunctional compounds, and materials with controlled properties [5–10]. These materials may be useful for the design of new-generation magnetic materials and active parts of sensors whose response is caused, for example, by a change in the optical, magnetic, and electric conductivity characteristics [11–15], displays [16], and heat-sensitive paints [17]. Compounds in which such changes are reversible are of particular interest for the above-indicated purposes. One of the approaches to the development of such systems is to generate stable radicals within transition metal complexes by oxidation or reduction of organic groups present in the ligands. The radical generation in a complex can affect its magnetic properties, since the unpaired electron of the radical may increase the magnetic susceptibility of the compound by increasing the total spin of the molecule [18, 19] or decrease the magnetic susceptibility due to antiferromagnetic coupling with the metal ion [20, 21]. In addition, the formation of a free radical may change the optical properties of the coordination compound due to the own color of the radical [22] or quenching of luminescence of another part of the molecule [23]. An important task of modern coordination and physical chemistry is to elucidate the effect of the structure of coordination compounds on the possibility of free radical generation in them. A great contribution to the coordination chemistry of metal–radical systems was made by Academician of the RAS V.I. Ovcharenko and co-workers, who elucidated the relationship between the structure and magnetic properties for 3*d* metal complexes with nitronyl nitroxide radicals [24, 25] and discovered the anomalous changes in the magnetic properties related to structural rearrangements for some of these complexes [26–28].

Previously, we predicted the possibility of generating a stable phenoxyl radical in coordination compounds containing a 2,6-di-*tert*-butylphenol moiety, that is, complexes with 2,6-di-*tert*-butyl-4-carboxyphenol [29] and 2,6-di-*tert*-butyl-4-(3,5-bis(4-pyridyl)pyridyl)phenol (L) [30, 31].

The goal of this work is to study the structure and magnetic properties of the binuclear copper(II) pivalate complex with the ligand L and to determine the conditions of formation of the phenoxyl radical in this compound.

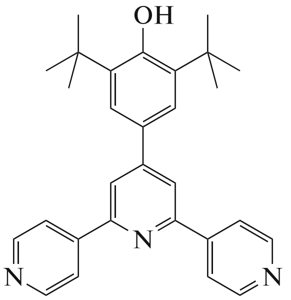

(L)

The paper describes the synthesis of a new complex, $Cu_2(Piv)_4(L)_2$, where Piv^- = pivalate, determination of its molecular and crystal structures at three temperatures, analysis of structural changes at different temperatures (dependences of $\chi_M T$ on T), electrochemical and magnetic properties of the complex, and the possibility of generating a long-lived radical upon UV radiation and oxidation with various oxidants.

EXPERIMENTAL

The new compounds were synthesized in air using commercially available reagents (Ukrorgsintez, Khimlaborreaktiv) and solvents (Ukrorgsintez), which were used as received. The initial complex **I** was obtained by a known procedure [32]. Ligand L was synthesized as described previously [30].

Synthesis of $Cu_2(Piv)_4(L)_2 \cdot 5.5H_2O \cdot 0.75CH_3CN$. A hot solution of $Cu(Piv)_2 \cdot 2H_2O$ (70 mg, 0.3 mmol) in CH_3CN (20 mL) was mixed with a hot solution of L (100 mg, 0.3 mmol) in CH_3CN (50 mL). Cooling of the mixture gave green crystals. After 24 h, the crystals were collected on a filter, washed with cold CH_3CN (5 mL), and dried in air. The yield was 140 mg (70%).

For $C_{79.5}H_{111.25}N_{6.75}O_{15.5}Cu_2$

Anal. calcd., %	C, 62.1	H, 7.30	N, 6.15
Found, %	C, 62.0	H, 7.05	N, 6.27

The composition of the bulk sample differed from the composition of single crystals that were stored under mother liquor and studied by X-ray diffraction. The temperature dependence of magnetic susceptibility was measured for the bulk sample $Cu_2(Piv)_4(L)_2 \cdot 5.5H_2O \cdot 0.75CH_3CN$.

Single-crystal X-ray diffraction study of $Cu_2(Piv)_4(L)_2 \cdot 5CH_3CN$ was performed on a Bruker Apex II diffractometer (CCD array detector, MoK_α, $\lambda = 0.71073$ Å, graphite monochromator) [33]. The structures were solved by direct methods and refined by full-matrix least-squares method in the anisotropic approximation for all non-hydrogen atoms. The hydrogen atoms at the carbon atoms of organic ligands were generated geometrically and refined in the riding model. The calculations were carried out by the SHELX program package [34] using OLEX 2 [35]. The structure of the complex determined at 296 K contained disordered solvent molecules, the contribution of which to the reflection intensity was estimated using the SQUEEZE/PLATON program [36]. Solution of the structure corresponding to 173 K resulted in location of two CH_3CN molecules with occupancy factor of 1 and one CH_3CN molecule with occupancy factor of 0.5 in the crystallographically non-equivalent moiety. The structure solved at 160 K contained one CH_3CN molecule with occupancy factor of 1 and two molecules with occupancy factor of 0.5. This difference is not obviously related to the desolvation of the single crystal on cooling and can be attributed to disordering of CH_3CN molecules, associated with their non-equilibrium reorientation on cooling of the single crystal and the quality of the particular crystal. One of the *tert*-butyl groups in the crystallographically non-equivalent moiety of the complex was disordered over two positions in all experiments. The crystallographic parameters are summarized in Table 1.

The full set of crystallographic parameters for $Cu_2(Piv)_4(L)_2 \cdot 5CH_3CN$ at different temperatures was deposited with the Cambridge Crystallographic Data Centre (nos. 2144104 (160 K), 2144105 (173 K), 2144106 (296 K); deposit@ccdc.cam.ac.uk or http://www.ccdc.cam.ac.uk/data_request/cif).

Elemental C,H,N analysis was performed using a Carlo Erba 1106 instrument. The ESR spectra were measured on a Bruker Elexsys II (X-range) spectrometer at room temperature.

The magnetic properties of the finely crystalline powder of $Cu_2(Piv)_4(L)_2 \cdot 5.5H_2O \cdot 0.75CH_3CN$ were measured using an PPMS-9 Quantum Design automated physical property measurement system. The temperature dependences of magnetization were determined in the temperature range $T = 9$–300 K in an $H = 5$ kOe external magnetic field. Corrections for the magnetic properties of the sample holder and for compound diamagnetism were applied using the Pascal scheme [37].

Cyclic voltammetry (CV) measurements were carried out using a PI-50 potentiostat with a platinum working electrode and an $Ag|AgNO_3$ reference electrode (0.1 M, CH_3CN). The electrode potential was

Table 1. Crystallographic data and X-ray experiment and structure refinement details for $Cu_2(Piv)_4(L)_2{\cdot}5CH_3CN$

Parameter	Value		
Temperature, K	160	173	296
Molecular formula	$C_{86}H_{110}N_{10}O_{10}Cu_2$	$C_{88}H_{113}N_{11}O_{10}Cu_2$	$C_{78}H_{98}N_6O_{10}Cu_2$
M	1570.92	1611.97	1406.70
System		Monoclinic	
Space group		$P2_1/c$	
a, Å	14.6615(13)	14.5609(17)	14.175(10)
b, Å	27.534(3)	27.392(3)	27.59(2)
c, Å	11.5852(11)	11.7917(13)	12.676(9)
β, deg	96.295(2)	96.501(2)	93.926(12)
V, Å^3	4648.7(7)	4672.9(9)	4947(6)
Z	2		
ρ(calcd.), g/cm^3	1.122	1.146	0.944
μ, mm^{-1}	0.514	0.513	0.476
F(000)	1668	1712	1492
Range of θ, deg.	2.26–28.27	1.59–25.03	2.06–24.71
Total number of reflections	38766	30788	31468
Number of unique reflections (R_{int})	11205 (0.1085)	8249 (0.1853)	8370 (0.1892)
Number of reflections with $I > 2\sigma(I)$	4933	4417	2753
R_1 $(I > 2\sigma(I))^a$	0.0495	0.0586	0.0544
wR_2 $(I > 2\sigma(I))^b$	0.0983	0.1393	0.1117
Residual electron density (max/min), e/Å^3	0.644/–0.410	0.837/–0.554	0.276/–0.261

[a] $R_1 = \Sigma||F_o| - |F_c||/\Sigma|F_o|$.

[b] $wR_2 = \{\Sigma[w(F_o^2 - F_c^2)^2]/\Sigma[w\left(F_o^2\right)^2]\}^{1/2}$.

determined with a solution of ferrocene (Fc); all potentials in the text are referred to the Fc^+/Fc pair. The Fc^+/Fc potential under experimental conditions was 35 mV, which is close to the expected value of 37 mV [38]. The concentration of a solution of $Cu_2(Piv)_4(L)_2$ in CH_3CN was 3×10^{-3} M; the potential sweep rate was 100 mV/s; other parameters and concentrations are indicated in the text.

The radical generation experiments were carried out as described previously [30]. The radicals were generated using two methods: UV irradiation and chemical oxidation by PbO_2 and $K_3[Fe(CN)_6]$. Solid samples of complex **I** were irradiated with UV light in a quartz tube under argon or oxidized with lead dioxide upon trituration with a drop of CH_2Cl_2. A solution of the complex in CH_2Cl_2 was oxidized with lead dioxide under argon (the reaction mixture was filtered, and the ESR spectrum of the filtrate was measured); and a suspension of solid $Cu_2(Piv)_4(L)_2$ was oxidized with an aqueous solution of $K_3[Fe(CN)_6]$ under argon (the reaction mixture was filtered, and the ESR spectrum of the solid residue was measured). The UV irradiation was performed with a Philips TUV-6 gas discharge lamp (λ_{max} = 256 nm; complete absorption of the UV radiation at λ_{max} < 185 nm). The concentrations of solutions and other parameters corresponded to the data reported in [30].

RESULTS AND DISCUSSION

The complex $Cu_2(Piv)_4(L)_2$ was prepared by the reaction of copper(II) pivalate with the ligand L at the Cu : L ratio of 1 : 1 in acetonitrile. According to single crystal X-ray diffraction, this compound crystallizes with six CH_3CN molecules per formula unit (not all CH_3CN molecules were reliably located during the crystal structure refinement), but during drying in air,

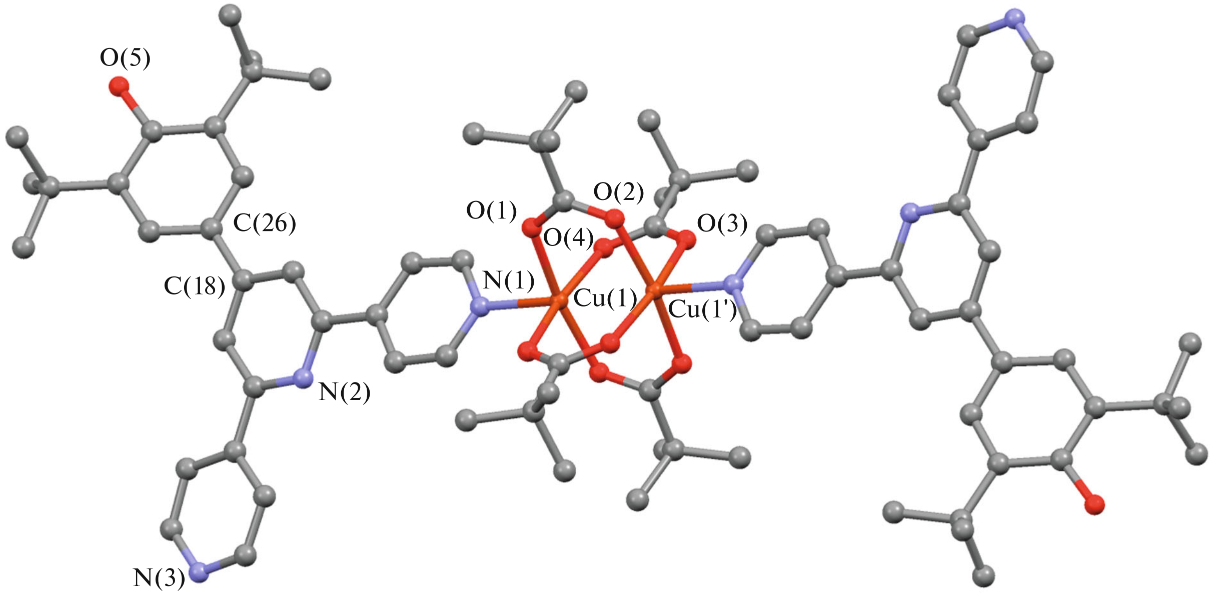

Fig. 1. Molecular structure of complex $Cu_2(Piv)_4(L)_2 \cdot 5CH_3CN$ at 160 K. Hydrogen atoms are omitted.

the greater part of captured acetonitrile is replaced by water.

The structure of $Cu_2(Piv)_4(L)_2 \cdot 5CH_3CN$ was determined by single crystal X-ray diffraction at three different temperatures: 160, 173, and 296 K. The complex has a molecular structure; the $Cu_2(Piv)_4(L)_2$ molecules crystallize as solvates with five acetonitrile molecules. The $Cu_2(Piv)_4(L)_2$ molecule is centrosymmetric and can be described as a binuclear copper(II) pivalate with a Chinese lantern geometry in which the axial positions at copper atoms are occupied by pyridine group nitrogens of L (Fig. 1). Hence, in each ligand L, only one terminal pyridine moiety is linked to the copper(II) ion. The structure of the complex is typical of binuclear copper carboxylates containing ligands with pyridine groups; the Cu–O and Cu–N bond lengths are in the expected ranges (Table 2) [39, 40]. As the temperature is lowered, the bond lengths, as expected, decrease, and the Cu...Cu length decreases from 2.6211(18) (296 K) to 2.5883(7) Å (160 K).

In the $Cu_2(Piv)_4(L)_2 \cdot 4CH_3CN$ crystal lattice, the hydrogen bonds between the pyridine nitrogen atoms and the hydroxy groups of the di-*tert*-butylphenol moieties of neighboring molecules give rise to nearly planar honeycomb type 2D layers (Fig. 2) with cavities of approximately 19 Å size (determined as the shortest distance between the hydrogen atoms of *tert*-butyl groups located on opposite sides of the cavity center). The presence of large cavities in the crystal lattice is consistent with the found differences between the solvate compositions of the bulk sample and the single crystal stored under the mother liquor.

The neighboring 2D layers in the crystal lattice of $Cu_2(Piv)_4(L)_2 \cdot 4CH_3CN$ are connected by π-stacking interactions between the aromatic rings of the ligands (Fig. 3). These layers are located in the planes parallel to vectors *b* and $(a - c)$ and perpendicular to vector $(a + c)$. As the temperature decreases from 296 to 160 K, the unit cell parameter *b* virtually does not change, whereas the parameter *a* increases by 3%, and *c* decreases by 9%. These changes are associated with

Table 2. Interatomic distances (Å) in $Cu_2(Piv)_4(L)_2 \cdot 5CH_3CN$

Distance	Temperature, K		
	160	173	296
Cu(1)–O(2)	1.959(2)	1.966(3)	1.976(4)
Cu(1)–O(4)	1.959(2)	1.972(3)	1.969(4)
Cu(1)–O(1)	1.965(2)	1.976(3)	1.966(4
Cu(1)–O(3)	1.966(2)	1.979(3)	1.972(4)
Cu(1)–N(1)	2.140(2)	2.150(3)	2.166(4)
Cu(1)...Cu(1)	2.5883(7)	2.5944(10)	2.6211(18)

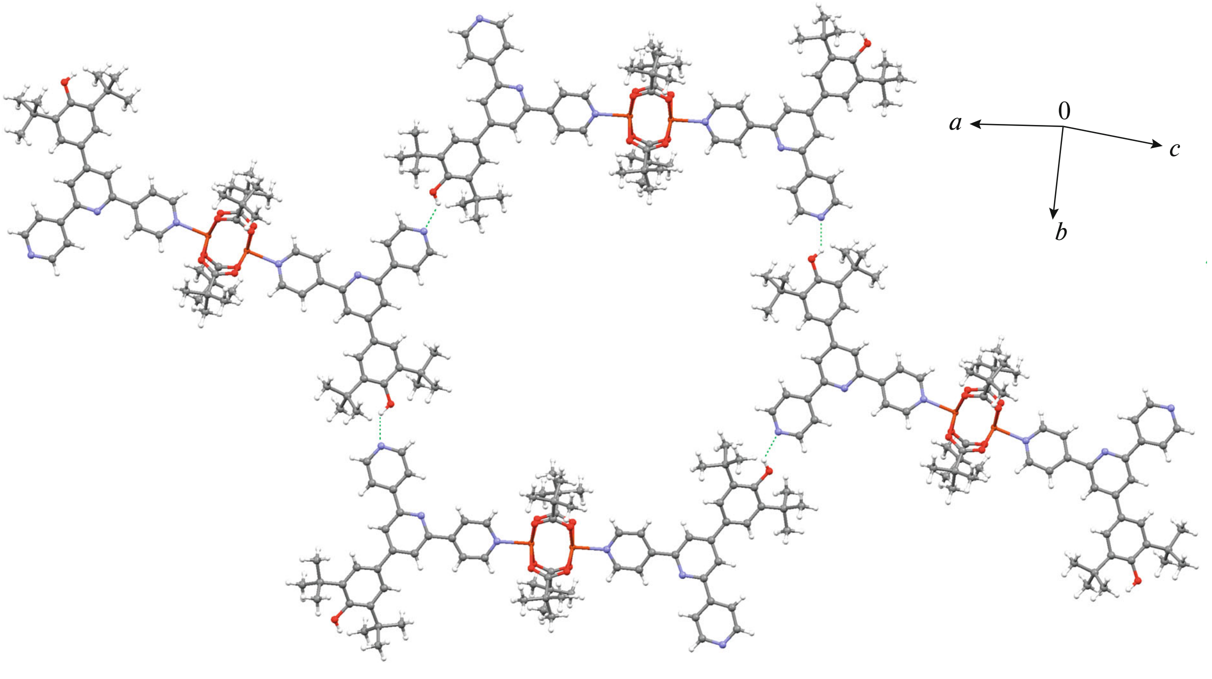

Fig. 2. Fragment of 2D layer in the crystal lattice of $Cu_2(Piv)_4(L)_2 \cdot 5CH_3CN$ formed by hydrogen bonds (shown by dashed lines). The drawing is based on X-ray diffraction data at 160 K. The CH_3CN molecules are omitted.

reorientation of molecules in the 2D layers, which is manifested most clearly as the crystal compression along vector ($a + c$). The shortest contacts between atoms in the aromatic rings involved in π-stacking decrease from 3.44 Å (at 296 K) to 3.31 Å (at 160 K): this decrease is reflected in crystal compression along the ($a + c$) direction. The N...O distances characterizing intermolecular hydrogen bonds within a 2D layer virtually do not change (they increase from 2.70 to 2.74 Å), which implies virtually invariable parameter b.

The $\chi_M T$ value (χ_M is the molar magnetic susceptibility per Cu_2 formula unit) of $Cu_2(Piv)_4(L)_2 \cdot 5.5H_2O \cdot 0.75CH_3CN$ at room temperature is 0.59 cm^3 K mol^{-1}, which is significantly lower than the value expected of a system consisting of two non-interacting copper(II) ions with $S = 1/2$ (0.75 cm^3 K mol^{-1} for $g = 2.0$). The significantly lower value than the expected one may be attributable to strong antiferromagnetic coupling in the binuclear $Cu_2(Piv)_4$ moiety, which is typical of copper(II) carboxylate dimer of this type [41]. At 2 K, $\chi_M T$ is 0.006 cm^3 K mol^{-1}; the low $\chi_M T$ value can be indicative of the absence of a metal-containing paramagnetic impurity. The unusual temperature dependence of $\chi_M T$ in the range from 2 to 300 K (Fig. 4), in particular, higher $\chi_M T$ compared to that expected of a binuclear copper(II) complex, can be interpreted as a superposition of $\chi_M T$ values of the binuclear moiety (Cu_2) and oxygen adsorbed in the pores of the crystal lattice of the complex [42].

The exchange interaction parameters in the $Cu_2(Piv)_4(L)_2$ dimer were calculated using a model based on Hamiltonian (1); it was suggested that the exchange interactions between neighboring blocks are negligibly low [43]:

$$\hat{H} = -2J\hat{S}_1\hat{S}_2. \qquad (1)$$

This approach made it possible to describe experimental data in the temperature range of 300–85 K with the parameters $J = -182(5)$ cm^{-1}, $g = 2.0$ (fixed), $tip = 8.2(5) \times 10^{-4}$ ($R^2 = 2.0 \times 10^{-4}$, $R^2 = \Sigma(\chi_M T_{calcd} - \chi_M T_{exp})^2/\Sigma(\chi_M T_{exp})^2$). Consideration of intermolecular interactions by the molecular field model did not result in a decrease in R^2.

According to CV data, no redox peaks were present in solutions of ligand L in the potential range from –1 to 2.3 V (in CH_3CN), in the potential range from –2 to 1.9 V (in DMF), and in the potential range from 0 to 3 V (in CH_2Cl_2) (in all cases, c(L) = 9×10^{-3} mol/L; 0.1 M NEt_4BF_4 supporting electrolyte; platinum electrode; the potentials are referred to Fc^+/Fc). No electrochemical activity of L was also detected in similar experiments for a solution of L in CH_3CN with the $NaClO_4$ supporting electrolyte (c = 0.1 mol/L) in the potential range from 0 to 2.5 V or in experiments with a platinum electrode with deposited L (a 0.1 M solution of NEt_4BF_4 in CH_3CN as the electrolyte) in the potential range from –1 to 2.3 V.

The cyclic voltammogram of a solution of $Cu_2(Piv)_4(L)_2$ in CH_3CN showed three successive fee-

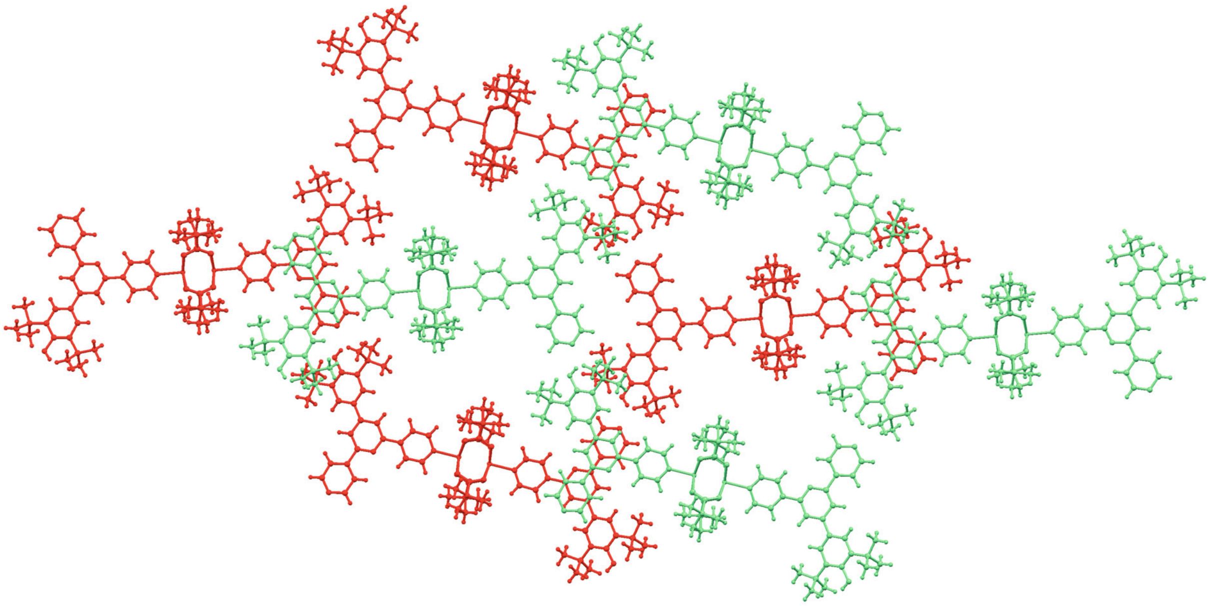

Fig. 3. Relative positions of neighboring 2D layers in the crystal lattice of $Cu_2(Piv)_4(L)_2{\cdot}4CH_3CN$ (the drawing is based on X-ray diffraction data at 160 K. The CH_3CN molecules are omitted).

bly pronounced anodic processes at potentials of 0.5, 0.9, and 1.2 V (versus Fc^+/Fc). On the basis of comparison with similar systems, the first peak can be assigned to irreversible oxidation of L to phenoxyl radical [29]. The assignment of the two subsequent processes is ambiguous: by analogy with the results of studies of the redox properties of copper(II) carboxylate dimers, these processes can refer to successive oxidations of two Cu^{2+} ions to Cu^{3+} ions within $Cu_2(Piv)_4$ [44]; however, it cannot be ruled out that they are due to irreversible oxidation of phenoxyl to quinone and oxidation of Cu^{2+} to Cu^{3+}, respectively.

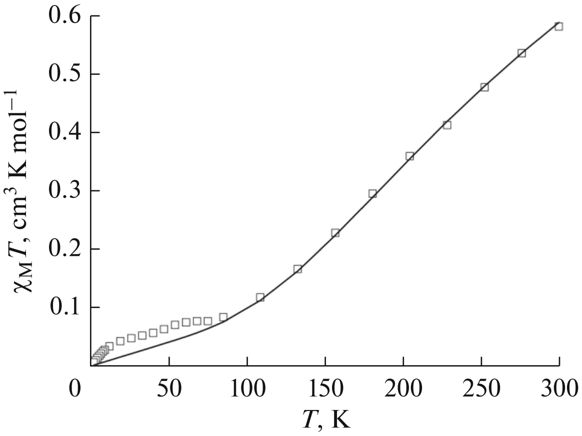

Fig. 4. Temperature dependence of $\chi_M T$ for $Cu_2(Piv)_4(L)_2{\cdot}5.5H_2O{\cdot}0.75CH_3CN$ (dots) and curve calculated using the parameters given in the text.

The generation of long-lived phenoxyl radicals upon irradiation of a solution of L or oxidation of L in solution with a suspension of PbO_2 was described in our previous study [30]. In order to investigate the possibility of generation of phenoxyl radicals upon the oxidation of $Cu_2(Piv)_4(L)_2$, we measured the ESR spectra of samples after irradiation in air or in vacuum and the spectra of reaction mixtures obtained by grinding this complex with PbO_2. It was found that these methods do not result in the formation of phenoxyl (at least, the amount of phenoxyl is too low for ESR detection). Meanwhile, the ESR signals with $g = 2.00$, which can be assigned to phenoxyl radicals, were found for a solution obtained after treatment of a CH_2Cl_2 solution of $Cu_2(Piv)_4(L)_2$ with a PbO_2 suspension (Fig. 5) and also for the solid sample obtained by vigorous stirring of a suspension of $Cu_2(Piv)_4(L)_2$ with an aqueous solution of $K_3[Fe(CN)_6]$. Note that solutions of binuclear copper(II) pivalates, unlike those of mononuclear complexes, exhibit no ESR signals for Cu^{2+} ions due to fast relaxation of the complex, resulting in a considerable broadening of the ESR signal [45].

The ESR signal of the sample obtained by treatment of the complex with a solution of $K_3[Fe(CN)_6]$ was detected repeatedly for at least one month. These results are consistent with the reported data on the oxidation of cobalt(II) complexes with L: treatment of solid samples of $[Co(L)Cl_2]_n$, $[Co_3(L)_2(OH)(Piv)_5]_n$, and $Co_3(H_2O)_4(L)_2Cl_6$ with a solution of $K_3[Fe(CN)_6]$ gave rise to a stable ESR signal, which could be assigned to the phenoxyl radical [30]. As in the case of previously described cobalt complexes, binding of L

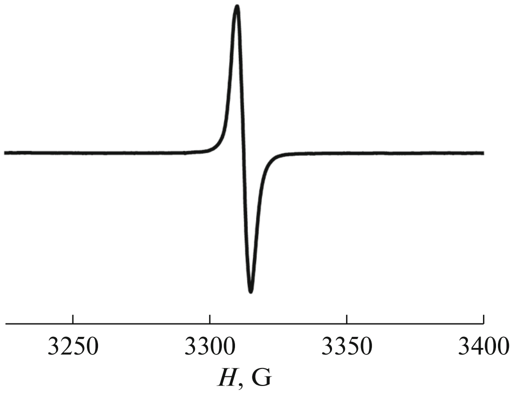

Fig. 5. ESR spectrum of a solution of $Cu_2(Piv)_4(L)_2$ after treatment with PbO_2 and filtration.

into the copper(II) complex markedly increases the radical stability (compared to that of the radical obtained from L in solution); this can be attributed to a lower rate of radical quenching reactions in the solid sample. However, oxidation of the solid sample is likely to give phenoxyl radicals only on the crystal surface.

Thus, the reaction of copper pivalate with L gave the complex $Cu_2(Piv)_4(L)_2$ (**I**) with a molecular structure. Due to specific packing, cavities are formed in the crystal lattice of **I**, which is manifested as both the ability of this complex to capture solvent molecules and appearance of a contribution of the captured oxygen in the dependence of $\chi_M T$ on T. The ligand L in $Cu_2(Piv)_4(L)_2$ can be oxidized both electrochemically and chemically, with the electrochemical oxidation being irreversible. The chemical oxidation of L gives a phenoxyl radical, which is markedly more stable when generated in a solid sample than when generated in a solution of L.

ACKNOWLEDGMENTS

A.V. Pavlishchuk, V.V. Pavlishchuk, V.N. Dorofeeva, S.V. Kolotilov, and K.S. Gavrilenko are grateful to the National Academy of Sciences of Ukraine (Project “Metal-Organic Frameworks and Polynuclear Complexes: Chemical Design, Structural Adsorption and Magnetic Luminescent Properties” based on the results of the joint competition of the National Academy of Sciences of Ukraine and the Russian Foundation for Basic Research of 2012). M.A. Kiskin, N.N. Efimov, V.V. Minin, and I.L. Eremenko are grateful to the Ministry of Education and Science of the Russian Federation for funding the research carried out within the framework of the State Assignment of the Kurnakov Institute of General and Inorganic Chemistry, Russian Academy of Sciences. The authors wish to thank A.S. Litvinenko (Pisarzhevsky Institute of Physical Chemistry, National Academy of Sciences of Ukraine) for help in cyclic voltammogram measurements.

CONFLICT OF INTEREST

The authors declare that they have no conflicts of interest.

REFERENCES

1. Rinehart, J.D. and Long, J.R., *Chem. Sci.*, 2011, vol. 2, p. 2078.
2. Craig, G.A. and Murrie, M., *Chem. Soc. Rev.*, 2015, vol. 44, p. 2135.
3. Liu, J.-L., Chen, Y.-C., and Tong, M.-L., *Chem. Soc. Rev.*, 2018, vol. 47, p. 2431.
4. D’Alessandro, D.M., *Chem. Commun.*, 2016, vol. 52, p. 8957.
5. Falcaro, P., Ricco, R., Doherty, C.M., et al., *Chem. Soc. Rev.*, 2014, vol. 43, p. 5513.
6. DeGayner, J.A., Jeon, I.-R., Sun, L., et al., *J. Am. Chem. Soc.*, 2017, vol. 139, p. 4175.
7. Feng, T., Ye, Y., Liu, X., et al., *Angew. Chem., Int. Ed. Engl.*, 2020, vol. 59, p. 21752.
8. Calbo, J., Golomb, M.J., and Walsh, A., *J. Mater. Chem. A*, 2019, vol. 7, p. 16571.
9. Sasaki, K., Yamate, H., Yoshino, H., et al., *Chem. Commun.*, 2020, vol. 56, p. 12961.
10. Li, H.-Y., Zhao, S.-N., Zang, S.-Q., et al., *Chem. Soc. Rev.*, 2020, vol. 49, p. 6364.
11. Li, Z., Wang, G., Ye, Y., et al., *Angew. Chem., Int. Ed. Engl.*, 2019, vol. 58, p. 18025.
12. Espallargas, M.G. and Coronado, E., *Chem. Soc. Rev.*, 2018, vol. 47, p. 533.
13. Zhou, Y., Yu, F., Su, J., et al., *Angew. Chem., Int. Ed. Engl.*, 2020, vol. 59, p. 18763.
14. Pasha, S.S., Yadav, H.R., Choudhury, A.R., et al., *J. Mater. Chem.*, 2017, vol. 5, p. 9651.
15. García-Valdivia, A.A., Pérez-Yáñez, S., Garcia, J.A., et al., *Sci. Rep.*, 2020, vol. 10, p. 8843.
16. Wang, Z., Yuan, X., Cong, S., et al., *ACS Appl. Mater. Interfaces*, 2018, vol. 10, p. 15065.
17. Kragt, A.J.J., Zuurbier, N.C.M., Broer, D.J., et al., *ACS Appl. Mater. Interfaces*, 2019, vol. 11, p. 28172.
18. Shimizu, D., Ide, Y., Ikeue, T., et al., *Angew. Chem., Int. Ed. Engl.*, 2019, vol. 58, p. 5023.
19. Woods, T.J., Stout, H.D., Dolinar, B.S., et al., *Inorg. Chem.*, 2017, vol. 56, p. 12094.
20. Kumar, P., Santalucia, D.J., Kaniewska-Laskowska, K., et al., *Inorg. Chem.*, 2020, vol. 59, p. 16178.
21. Alexandropoulos, D.I., Vignesh, K.R., Xie, H., et al., *Chem. Commun.*, 2020, vol. 56, p. 9122.
22. Liu, J., *Dyes Pigm.*, 2019, vol. 160, p. 476.
23. Tansakul, C., Lilie, E., Walter, E.D., et al., *J. Phys. Chem. C*, 2010, vol. 114, p. 7793.
24. Tretyakov, E.V. and Ovcharenko, V.I., *Russ. Chem. Rev.*, 2009, vol. 78, p. 971.
25. Ovcharenko, V., *Stable Radicals: Fundamentals and Applied Aspects of Odd-Electron Compounds*, Hicks, R.G., Ed., New York: Wiley, 2010, p. 461.
26. Ovcharenko, V.I., Maryunina, K.Yu., Fokin, S.V., et al., *Russ. Chem. Bull.*, 2004, vol. 53, p. 2406.

27. Fedin, M., Veber, S., Gromov, I., et al., *Inorg. Chem.*, 2007, vol. 46, p. 11405.
28. Romanenko, G.V., Maryunina, K.Y., Bogomyakov, A.S., et al., *Inorg. Chem.*, 2011, vol. 50, p. 6597.
29. Yakovenko, A.V., Kolotilov, S.V., Addison, A.W., et al., *Inorg. Chem. Commun.*, 2005, vol. 8, p. 932.
30. Dorofeeva, V.N., Pavlishchuk, A.V., Kiskin, M.A., et al., *ACS Omega*, 2019, vol. 4, p. 203.
31. Dorofeeva, V.N., Lytvynenko, A.S., Kiskin, M.A., et al., *Book of Abstracts of VI International Conference* "*High-Spin Molecules and Molecular Magnets,*" Rostov-on-Don, 2012, p. 92.
32. Denisova, T.O., Amel'chenkova, E.V., Pruss, I.V., et al., *Russ. J. Inorg. Chem.*, 2006, vol. 51, no. 7, p. 1020.
33. *SMART (control) and SAINT (integration) Software. Version 5.0*, Madison: Bruker AXS Inc., 1997.
34. Sheldrick, G.M., *Acta Crystallogr., Sect. C: Struct. Chem.*, 2015, vol. 71, p. 3.
35. Dolomanov, O.V., Bourhis, L.J., Gildea, R.J., et al., *J. Appl. Crystallogr.*, 2009, vol. 42, p. 339.
36. Spek, A.L., *PLATON. A Multipurpose Crystallographic Tool*, Utrecht: Utrecht University, 2006.
37. Kahn, O., *Molecular Magnetism*, Weinheim: VCH, 1993.
38. Pavlishchuk, V.V. and Addison, A.W., *Inorg. Chim. Acta*, 2000, vol. 298, p. 97.
39. Dorofeeva, V.N., Mishura, A.M., Lytvynenko, A.S., et al., *Theor. Exp. Chem.*, 2016, vol. 52, p. 111.
40. Polunin, R.A., Burkovskaya, N.P., Kolotilov, S.V., et al., *Izv. Akad. Nauk. Ser. Khim.*, 2014, vol. 1, p. 252.
41. Reger, D.L., Debreczeni, A., Smith, M.D., et al., *Inorg. Chem.*, 2012, vol. 51, p. 1068.
42. Kawamura, K., Makishima, Y., and Ochiai, Y., *Carbon Sci. Tech.*, 2009, vol. 2, p. 73.
43. Kalinnikov, V.T. and Rakitin, Yu.V., *Vvedenie v magnetokhimiyu. Metod staticheskoi magnitnoi vospriimchivosti v khimii* (Introduction to Magnetochemistry. Static Magnetic Susceptibility Method in Chemistry), Moscow: Nauka, 1980.
44. Fomina, I., Dobrokhotova, Z., Aleksandrov, G., et al., *Polyherdron*, 2010, vol. 29, p. 1734.
45. Carrington, A. and McLachlan, A.D., *Introduction to Magnetic Resonance: With Applications to Chemistry and Chemical Physics* (*Science Books*), Chapman and Hall, 1979.

Translated by Z. Svitanko